

PAPER • OPEN ACCESS

Charge, transport, conductivity and Seebeck coefficient in pristine and TCNQ loaded preferentially grown metal-organic framework films

To cite this article: Xin Chen *et al* 2022 *J. Phys.: Condens. Matter* **34** 404001

View the [article online](#) for updates and enhancements.

You may also like

- [Influence of TCNQ Loading on the Mechanical Properties of Metal-Organic Framework Films](#)
Yousuf Mohammed, Xin Chen, Zeinab Mohamed Hassan *et al.*
- [Seebeck Coefficient Measurements of Polycrystalline and Highly Ordered Metal-Organic Framework Thin Films](#)
Xin Chen, Zhengbang Wang, Zeinab Mohamed Hassan *et al.*
- [Review—Recent Advance in Multi-Metallic Metal Organic Frameworks \(MM-MOFs\) and Their Derivatives for Electrochemical Biosensor Application](#)
Muhammad Rezki, Ni Luh Wulan Septiani, Muhammad Iqbal *et al.*



IOP | ebooks™

Bringing together innovative digital publishing with leading authors from the global scientific community.

Start exploring the collection—download the first chapter of every title for free.

Charge transport, conductivity and Seebeck coefficient in pristine and TCNQ loaded preferentially grown metal-organic framework films

Xin Chen¹, Kai Zhang^{1,2}, Zeinab Mohamed Hassan³, Engelbert Redel³ 
and Helmut Baumgart^{1,2}

¹ Dept. Electrical and Computer Engineering, Old Dominion University, Norfolk, VA 23529, United States of America

² Applied Research Center, Newport News, Thomas Jefferson National Accelerator Lab, Virginia 23606, United States of America

³ Institute of Functional Interfaces (IFG), Karlsruhe Institute of Technology (KIT), Hermann-von-Helmholtz-Platz 1, 76344 Eggenstein-Leopoldshafen, Germany

Received 1 August 2020, revised 12 November 2020

Accepted for publication 17 February 2021

Published 9 August 2022



Abstract

This investigation on metal-organic framework (MOF) HUKUST-1 films focuses on comparing the undoped pristine state and with the case of doping by TCNQ infiltration of the MOF pore structure. We have determined the temperature dependent charge transport and *p*-type conductivity for HKUST-1 films. Furthermore, the electrical conductivity and the current–voltage characteristics have been characterized in detail. Because the most common forms of MOFs, bulk MOF powders, do not lend themselves easily to electrical characterization investigations, here in this study the electrical measurements were performed on dense, compact surface-anchored metal-organic framework (SURMOF) films. These monolithic, well-defined, and (001) preferentially oriented MOF thin films are grown using quasi-liquid phase epitaxy (LPE) on specially functionalized silicon or borosilicate glass substrates. In addition to the pristine SURMOF films also the effect of loading these porous thin films with TCNQ has been investigated. Positive charge carrier conduction and a strong anisotropy in electrical conduction was observed for highly oriented SURMOF films and corroborated with Seebeck coefficient measurements. Van der Pauw four-point Hall sample measurements provide important insight into the electrical behavior of such porous and hybrid organic–inorganic crystalline materials, which renders them attractive for potential use in microelectronic and optoelectronic devices and thermoelectric applications.

Keywords: thin films, MOFs, charge transport, conductivity, Seebeck coefficient

(Some figures may appear in colour only in the online journal)



Original content from this work may be used under the terms of the [Creative Commons Attribution 4.0 licence](https://creativecommons.org/licenses/by/4.0/). Any further distribution of this work must maintain attribution to the author(s) and the title of the work, journal citation and DOI.

Organic materials with tunable electrical properties are of considerable interest for the next generation of microelectronics, optoelectronic and thermoelectric devices. In the quest for new materials, hybrid compounds or organic heterolayers are being increasingly investigated regarding these potential applications [1]. In this study, we focus on compact metal-organic framework (MOF) films, which are another class of hybrid material. MOFs are highly tunable and porous, and are also known as porous coordination polymers [2]. Metal-organic frameworks are formed by connecting organic linkers via inorganic metal (or metal/oxo) clusters [3, 4]. Due to their crystallinity, their thermal stability of typically up to 250 °C and their open porous framework structure, this class of solids is highly adjustable and possesses interesting properties, which can be modulated and custom tailored.

For example, the sizes of the pores within MOFs have been reported to be highly tunable [5], and pore widths up to 10 nm have been reported [6], yielding porous solids with extremely low densities. For the time being, bulk MOF powders constitute the de-facto standard modification of MOF materials. The typical product of the most commonly applied solvothermal synthesis method yields loosely packed bulk MOF powders, containing MOF crystallites with a widespread size distribution up to the mm range. Determining the electrical properties and characteristics of this class of solid porous materials with conventional methods for powders is difficult and challenging. However, meaningful electrical characteristics can be measured by employing compact highly oriented crystalline and monolithic thin films of MOFs instead, which can be grown by quasi liquid phase epitaxy (LPE) [6]. Such monolithic and dense highly oriented MOF thin films are referred to as surface-anchored metal-organic framework (SURMOF) films. The superior elastic and mechanical properties of SURMOF films have already been reported for single layered materials as well as in multilayered architectures [7, 8].

Therefore, compact highly oriented SURMOF films offer a clear advantage in this context. A number of different techniques and methods are currently known for preparing polycrystalline MOF coatings [9]; in addition, the deposition of MOF [10] materials has been described for the fabrication of electrical and microelectronic devices [11, 12]. It is rather obvious that the electrical properties of porous MOFs/SURMOFs change when guest molecules are loaded into the pores of the framework. The first studies of this type were reported by Dragässer *et al*, for the case of loading ferrocene inside monolithic HKUST-1 SURMOF thin films [13], where the acronym HKUST denotes ‘Hong Kong University of Science & Technology’, that originally publicized this MOF structure. Later, Talin *et al* found that after loading TCNQ (Tetracyanoquinodimethane) molecules into the framework of HKUST-1, the electrical conductivity increased over six orders of magnitude with values up to 7 S m^{-1} in air [14].

First models have suggested that the conductivity arises from redox-active TCNQ guest molecules linking the copper paddlewheels within the open pores of HKUST-1. Charge transport between the TCNQ guests has been recently described and theoretically investigated by a second order process [15]. In this experimental study, it was also pointed

out that inconsistencies exist between the electron-conducting mechanism proposed by these authors and the experimentally established positive sign of the Seebeck-coefficient [16], which points to a *p*-type conducting mechanism.

Here, we investigate the electrical properties of pristine HKUST-1 and TCNQ loaded compact HKUST-1 SURMOF films by *I*–*V* characteristics and four-point Van der Pauw Hall configuration measurements. The compact MOF thin films were grown on pretreated Si and nonconductive borosilicate and quartz substrates using quasi LPE in conjunction with a spray process already reported in our previous studies [6]. This process yields film thicknesses in the range of ≈ 40 –100 nm, depending on the number of spraying cycles used [17]. SURMOF films were characterized using x-ray diffraction (XRD) and IRRAS measurements. Morphological studies through scanning electron microscope (SEM) cross-sectional measurements have been applied to check for continuity, homogeneity, and compactness of the monolithic SURMOF thin films, as well as to detect possible meso/macro porosity within the quasi epitaxially grown SURMOF films. Recently, a number of alternative procedures have been developed for the fabrication of MOF thin films, including dipping, spin-coating as well as electrochemical techniques [4, 17]. However, it has been difficult to achieve high quality oriented MOF thin films with low defect density using the above-described methods. In contrast, it is possible to growth very compact and highly oriented SURMOF thin films of high morphological quality and low surface roughness by employing the controlled process of quasi LPE on functionalized Si/Au substrates [11]. Excellent quality of highly oriented or polycrystalline HKUST-1 thin films can be achieved on modified silicon and quartz substrates, which is an essential prerequisite for enabling good electrical contacts and horizontal/in-plane electrical conductivity measurements in order to obtain reproducible results. SURMOF films synthesized from other MOF systems have been studied in previous works with regard to their mechanical [7], optical/photonic [18], magnetic [19], or electrical [20] behavior, which are key properties for the desired functionality.

HKUST-1 is constructed from Cu^{++} dimers and benzenetricarboxylate (BTC) units which form a crystalline, 3D porous structure with a pore diameter of 1.2 nm, where the available pores allow the loading or storage of guest molecules for example TCNQ inside the MOF structure (see the schematic chemical model of figure 1(A)). HKUST-1 MOF films used in this study were grown on plasma-treated silicon and glass substrates by LPE spray method [9], in which the metal-containing solution [1 mmol $\text{Cu}(\text{OAc})_2$] and the linker solution [0.1 mmol BTC] are sprayed subsequently on the pretreated Si, borosilicate glass or quartz substrate. For this study, the standard spray procedure was modified by omitting the rinsing process with pure ethanol in order to achieve random polycrystalline, non-oriented MOF films, which is a prerequisite for horizontal/in-plane conductivity measurements due to the observed anisotropy in highly oriented quasi epitaxial SURMOF films [21, 22]. In an earlier report such highly oriented crystalline SURMOF film have been successfully used for resistive switching between film surface and film backside electrodes using aligned MOF pores for charge transport [11].

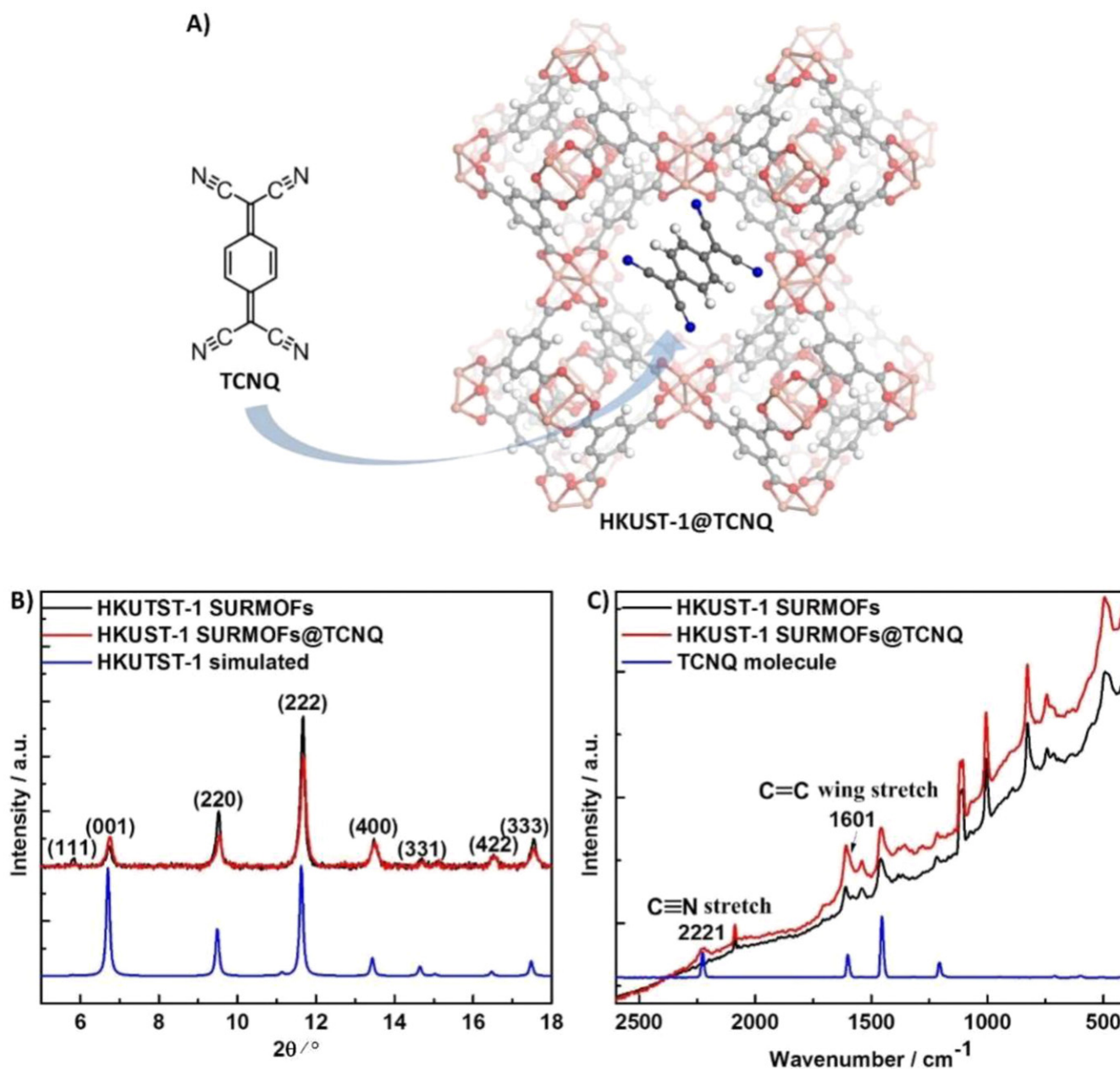


Figure 1. (A) Schematic illustration depicting the structure of HKUST-1 SURMOF films, where the pores are loaded with TCNQ (TCNQ, tetracyanoquinodimethane). (B) Plot of x-ray diffraction (XRD) patterns of pristine random polycrystalline HKUST-1 SURMOF films shown in black, while the experimental data of the HKUST-1 SURMOF films loaded with TCNQ are plotted in red. For comparison, a simulated HKUST powder diffraction plot is shown in blue color. It is apparent that the loading of the HKUST-1 pores with TCNQ did not alter or disturb the crystal structure. (C) Plot of Raman spectrum of pristine HKUST-1 SURMOF films versus the HKUST-1 SURMOF films loaded with TCNQ in the pores, reference [23].

Next to electrical charge transport in MOF thin films, new developments have been recently reported for their thermal conductivity [23, 24].

The crystalline nature of the resulting HKUST-1 SURMOF films was verified by XRD. A typical XRD diffraction pattern is displayed in figure 1(B) (black curve). The XRD data clearly demonstrate the presence of random polycrystalline HKUST-1 MOF films with random orientation of the individual crystallites. The experimental XRD data compare well with the simulated HKUST-1 MOF powder diffraction pattern. The loading of TCNQ into the HKUST-1 MOFs was carried out

by a liquid-phase procedure, where the as-synthesized MOF thin film was first activated by annealing at 60 °C for 4 h to remove any remaining solvent stored in the pore of MOF materials. Subsequently, the samples were immersed into an ethanolic TCNQ solution (2 mM) for 72 h at room temperature. Finally, the sample was rinsed using pure ethanol to remove the TCNQ molecules adsorbed on the surface. To ascertain the successfully loading of TCNQ molecules, Raman spectra of the sample before and after loading as well as the drop cast TCNQ molecule on a gold substrate were recorded and are displayed in figure 1(C). The Raman spectra recorded

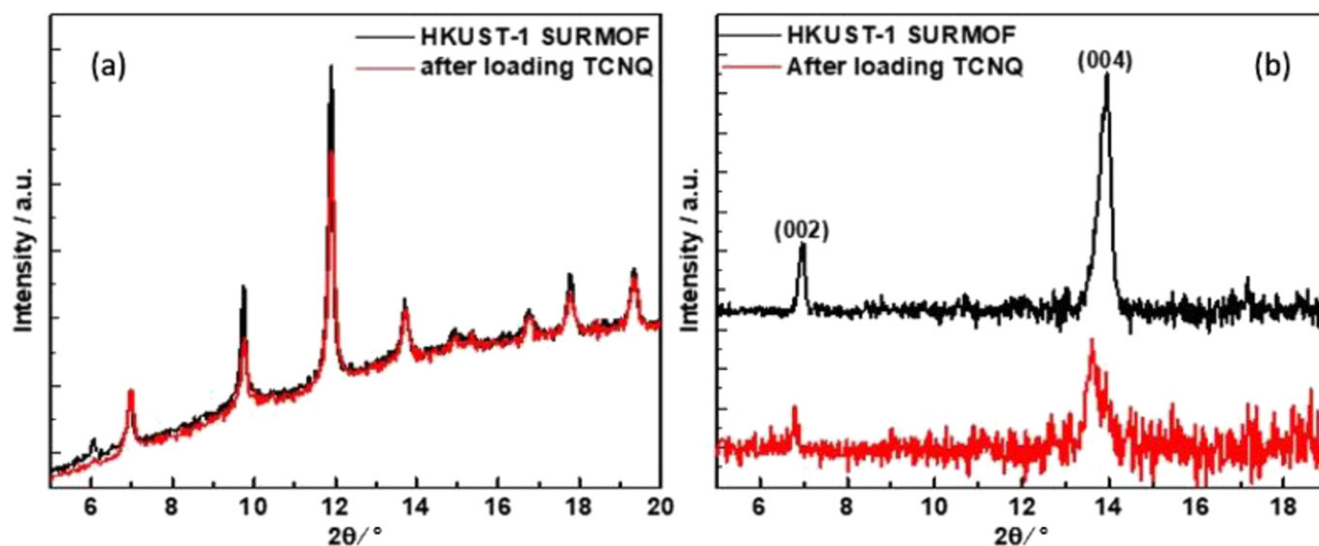


Figure 2. XRD plots highlighting the difference between quasi epitaxial growth of preferentially oriented SURMOF film versus polycrystalline XRD signature, (a) random polycrystalline HKUST-1 SURMOF films before (black line) and after (red line) TCNQ loading grown on thermal oxidized SiO_2/Si wafer, (b) preferentially (001) oriented crystalline HKUST-1 SURMOF films before (black line) and after (red line) TCNQ loading obtained by growth on SAMs functionalized Au surface or on quartz. With permission from reference [22].

after loading provide a clear signature of TCNQ molecules, such as the peak at 2221 cm^{-1} and 1601 cm^{-1} wavenumbers. These Raman signals were assigned to the C and N triple bond stretch and C and C double bond wing stretch, respectively and provide a signature for the presence of TCNQ. The other Raman-bands related to the HKUST framework showed no changes after loading, which suggests that the infiltration with TCNQ did not change or deteriorate the original HKUST-1 SURMOF host structure. XRD data received from the sample after loading with TCNQ provided additional evidence that the thin films are still crystalline. The slight change of relative XRD intensity is attributed to the form factor change after loading the guest molecule into the porous crystal structure. Figures 2(a) and (b) highlights the difference between quasi-epitaxial growth of preferentially oriented SURMOF films grown on quartz versus polycrystalline SURMOF films grown on thermal oxidized SiO_2/Si wafer [24]. All chemical precursors used in this work are commercially available from sigma Aldrich and the *p*-type silicon substrates were received from Silchem Handelsgesellschaft GmbH, Germany.

In this study, HKUST-1 SURMOF films were quasi liquid-phase epitaxially (LPE) grown with a preferential crystal orientation on functionalized interfaces, which consisted of a thin Au film followed by a self-assembled monolayer (SAM layer) on silicon wafers covered with a native oxide layer. The LPE spray method has already been described elsewhere [4, 17], where the metal-containing solution [1 mmol $\text{Cu}(\text{OAc})_2$] and the linker solution [0.1 mmol BTC] are sprayed alternately on the Si or borosilicate substrate.

The desired MOF film thickness can be adjusted using a number of distinct LPE spray cycles; e.g., 15, 25, 30 and 45 spray cycles for HKUST-1 SURMOF films resulting in a total film thickness of ~ 40 , ~ 60 , ~ 70 and ~ 100 nm as illustrated in the SEM cross-sections of figure 3. After the quasi

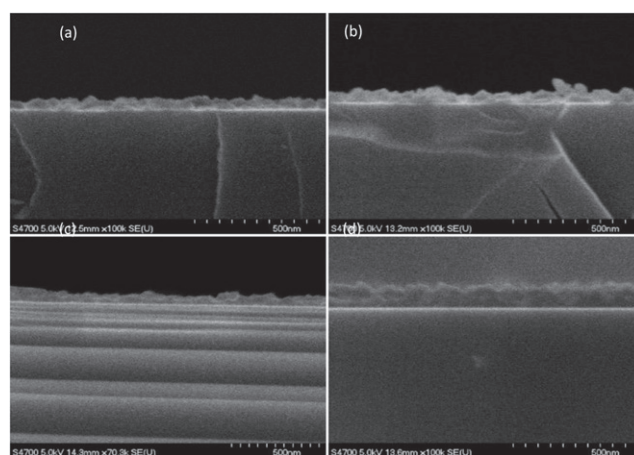


Figure 3. FE-SEM cross-sectional micrographs of SURMOF HKUST-1 films with thickness of (a) 40 nm, (b) 60 nm, (c) 70 nm, and (d) 100 nm on Silicon substrates references [23, 28].

epitaxial growth of the MOF films, all samples were characterized using XRD with a D8-Advance Bruker AXS diffractometer with $\text{Cu K}\alpha$ radiation ($\lambda = 1.5418\text{ \AA}$) in $\theta/2\theta$ geometry equipped with a position sensitive detector. XRD data have been recorded for all samples before and after loading the pores with TCNQ. Morphology studies were performed using cross-sectional images with a Hitachi S 4700 FE-SEM operated at 5 kV for MOF films on silicon substrates on an Al-SEM cross-section holder shown in figure 3 and also for planar view SURMOF samples shown in figures 4 and 5.

1. Electrical measurements

1.1. Seebeck coefficient

To elucidate the electrical characteristics of SURMOF films we conducted Seebeck coefficient measurements,

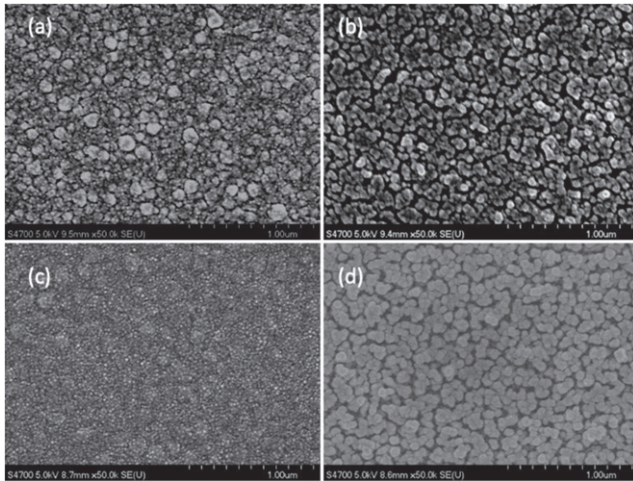


Figure 4. Planar view FE-SEM micrographs of MOF films grown on borosilicate glass substrates displaying a different MOF morphology of very loosely stacked MOF grains with very noticeable gaps between individual MOF grains (a) 10 cycles pristine MOF (b) 10 cycles TCNQ loaded MOF (c) 40 cycles MOF (d) 40 cycles MOF with TCNQ loading.

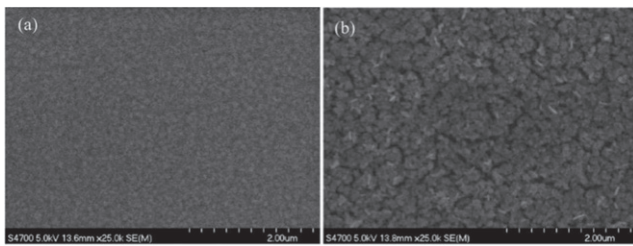


Figure 5. Top-down planar view FE-SEM micrographs of (a) pristine and (b) TCNQ loaded random polycrystalline SURMOF HKUST-1 thin film synthesized on hydroxyl terminated SiO_2/Si substrate.

current–voltage (I – V) characteristics and Van der Pauw four-point Hall configuration measurements. First, we measured the Seebeck coefficient S as a function of temperature for random polycrystalline SURMOF films infiltrated with TCNQ and compared the results with the case of preferentially (001) oriented SURMOF films with TCNQ loading, referred to in the XRD plots of figure 2(b). During our Seebeck measurements of dense highly oriented crystalline SURMOF films a strong anisotropy of electrical conduction was observed between preferentially oriented quasi liquid epitaxial SURMOF films versus random polycrystalline MOF films. Figure 6(a) plots the temperature dependence of the measured Seebeck coefficient of quasi-epitaxial highly oriented SURMOF films with and without (pristine) TCNQ infiltration. In both cases for pristine and loaded MOFs, the horizontal Seebeck coefficient of highly oriented SURMOF films is hardly measurable fluctuating around $0 \mu\text{V K}^{-1}$ and in the noise level over the entire temperature testing range from 295 K to 350 K. However, for the case of random polycrystalline SURMOF films grown on thermal oxidized Si substrates with thick 484 nm isolation SiO_2 the horizontal Seebeck coefficient is measurable over the temperature range between 290 K and 350 K. The

maximum measured Seebeck coefficient of TCNQ loaded polycrystalline MOFs with film thickness of 200 nm and TCNQ infiltration was $422.32 \mu\text{V K}^{-1}$ at 350 K, see figure 6(b). We attribute these results to the fact that SURMOF films grown on SAM functionalized gold coated Si substrates exhibit a strong preferential orientation along the (001) direction [4]. For such highly preferentially oriented films a previous study has demonstrated good charge carrier transport only through the vertical direction with surface top contacts and backside contacts [11] while no carrier transport takes place in the horizontal in-plane direction parallel to the surface. MOF films grown directly on thermally oxidized Si substrates without the use of SAM functionalized Au layers are subject to heterogeneous nucleation resulting into random polycrystalline MOF films. The isotropic nature of these random polycrystalline MOF films enabled charge carrier transport via all directions. For this reason, the measured horizontal Seebeck coefficient of highly oriented SURMOF films parallel to the surface was negligibly small around $0 \mu\text{V K}^{-1}$, while the Seebeck coefficient of random oriented polycrystalline MOF films measured fairly high values. It is noteworthy to point out that the measured Seebeck coefficient of polycrystalline SURMOF films was positive, thereby indicating the SURMOF films are p -type, where the majority charge carriers are holes. Our measurements are consistent with literature work [16]. The positive Seebeck coefficient of TCNQ loaded polycrystalline MOF films increases linearly from $342.39 \mu\text{V K}^{-1}$ to $422.32 \mu\text{V K}^{-1}$ as the temperature rises from 290 K to 350 K, because thermal activation generates more charge carriers contributing to the Seebeck coefficient at higher temperatures. The plots of the temperature dependent Seebeck coefficient of the pristine MOF films versus the TCNQ loaded films exhibit roughly the same slope and tendency over the temperature range between 290 K and 330 K and are parallel shifted by approximately $50 \mu\text{V K}^{-1}$. The Seebeck coefficient S is inversely proportional to electrical conductivity σ and charge carrier density n . This explains why the higher electrical conductivity of TCNQ loaded SURMOF samples results necessarily in lower Seebeck coefficient values. The Mott relationship stipulates that the lower carrier density of pristine undoped polycrystalline MOF films results in higher Seebeck coefficients, while conversely the TCNQ loading of the pores effectively enhances the charge carrier density and electrical conductivity of isotropic polycrystalline MOF films. Because of the inverse relationship with carrier density this fact leads to a lower Seebeck coefficient.

1.2. Thin-film electrical conductometry

For further investigation of the electrical properties of SURMOF films, the I – V -characteristic curves of preferentially (001) oriented MOFs grown on Au and SAM functionalized Si substrate or on quartz were measured and compared to polycrystalline MOFs grown on native oxide covered Si substrates and on borosilicate glass.

All the electrical properties measurements were performed with an Ecopia Hall effect measurement system (HMS-5300) using a symmetrical four-point Van der Pauw Hall configuration sample 25. The Hall system is equipped with a

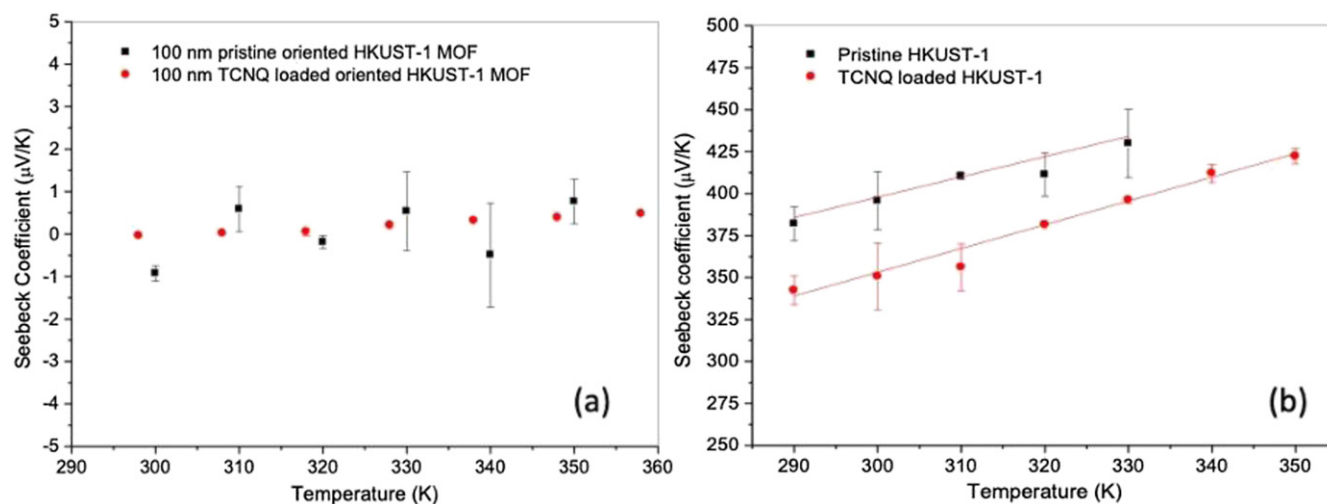


Figure 6. (a) Seebeck coefficient measurements as function of temperature of LPE highly oriented HKUST-1 films with a thickness of 100 nm, which were prepared with and without TCNQ loading. For the case of the highly oriented SURMOF film the Seebeck coefficient oscillates around zero within the margin of error. (b) However, in the case of random polycrystalline SURMOF films the Seebeck coefficient is measurable and increases as a function of temperature of LPE polycrystalline HKUST-1 thin film with a thickness of 200 nm. Pristine HKUST-1 SURMOF films exhibit a higher Seebeck coefficient compared to TCNQ loaded samples, references [23, 28].

0.556 T permanent magnet, and a variable temperature test is available from 80 K to 550 K. Liquid nitrogen was used to cool down the system to the desired initial test temperature. In the experiment, square-shaped samples in size of $1\text{ cm} \times 1\text{ cm}$ with four symmetrical Au surface contacts on the corners were prepared for testing. Initially, for the first set of electrical tests the Au electrodes were sputter deposited directly on the surface of the MOF film on the four corners of the sample through use of a shadow mask in a Van der Pauw sample arrangement. The four Au surface contacts were of equal size and less than $1 \times 1\text{ mm}^2$ in area and with a thickness of 150 nm. Figure 7(b) displays a photographic image of the Hall measurement stage mounted a sample with the four sputtered Au contacts using a Van der Pauw Hall configuration sample. However, ongoing analysis revealed that any surface Au contacts fabricated by either sputtering, thermal evaporation or e-beam evaporation causes deterioration of the hybrid SURMOF material and physical surface damage complicating the evaluation of test results. For this reason, we resorted to bottom Au contacts. For this endeavor we designed a shadow mask for square samples, which allows to sputter the Au contacts through the mask openings to fabricate the four corner bottom contacts. This way we made sure to protect the physical integrity of the SURMOF films by always using bottom Au contacts with a mask and subsequently synthesized the SURMOF films on top of the pre-deposited gold contacts. These protective measures ensure a pristine condition of the surface morphology and integrity of the SURMOF films. Figure 7(a) provides a schematic of the sample stage pre-structured with four bottom Au contacts illustrating the design of the test sample, while figure 7(b) provides a photographic image of the Hall Effect measurement stage with square SURMOF sample with sputtered Au bottom contacts in the four corners for a Van der Pauw configuration.

The characteristic $I-V$ curves of polycrystalline SURMOF films on borosilicate glass substrates with and without TCNQ

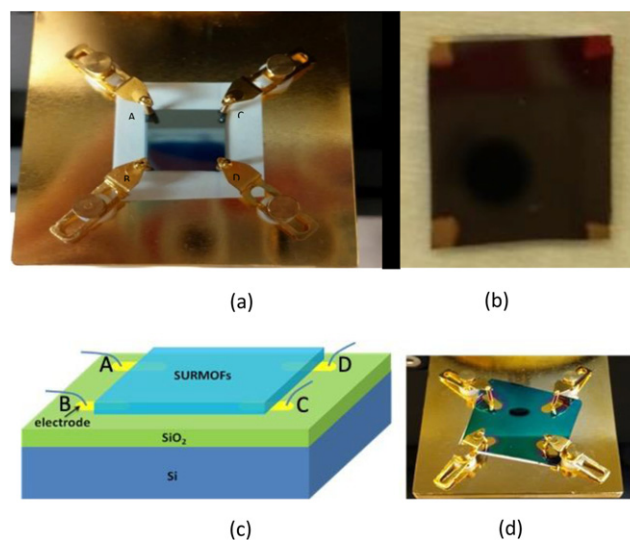


Figure 7. (a) Photographic image of Hall sample measurement stage showing the mounted test device. (b) Photograph image of a square SURMOF sample with sputtered Au contacts on the surface of the MOF film in the four corners for a Van der Pauw Hall sample configuration. (c) Schematic of the MOF samples with four bottom contacts. (d) Hall Effect measurement stage with square MOF sample with sputtered Au bottom contacts in the four corners for a Van der Pauw configuration, reference [28].

infiltration are displayed in the plots of figure 8. The measurements demonstrate that the TCNQ loading is boosting lateral electrical conductivity in the film and results in a measurable $I-V$ curve, while the pristine non-loaded MOF films exhibit practically zero conductivity. Lateral in-plane current-voltage measurements were conducted on the Van der Pauw samples between two Au contacts and were repeated for the following contact pairs: AB, BC, CD and between contacts DA. Clearly the TCNQ infiltration helps the SURMOF films on borosilicate glass to attain a meaningful conductivity, and the linear

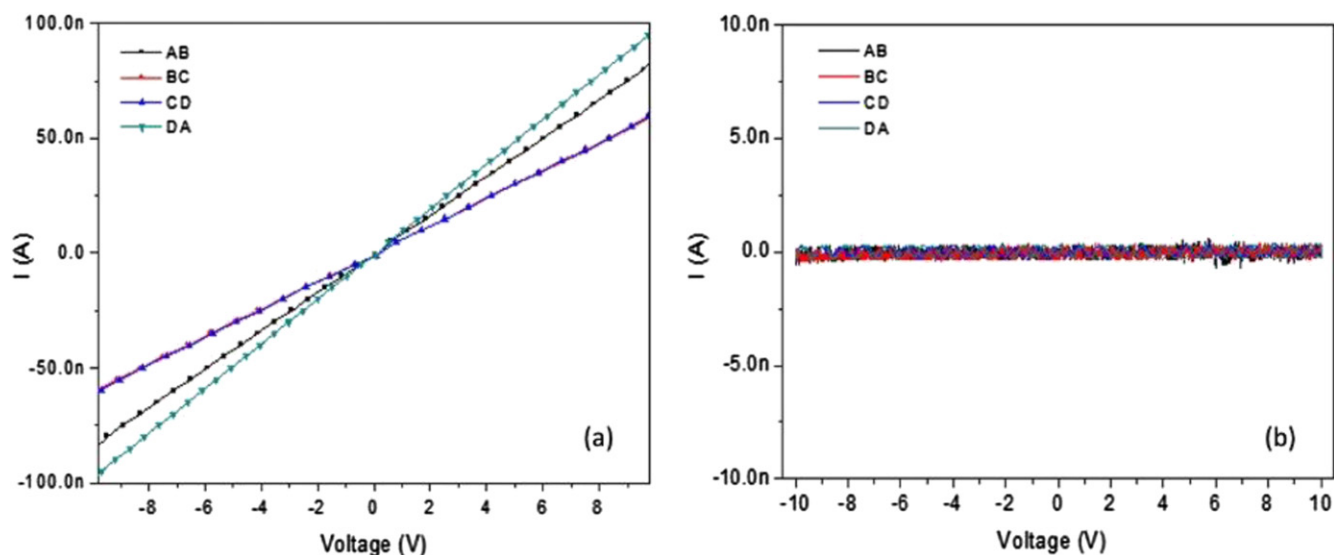


Figure 8. (a) Plot of I - V characteristics of TCNQ loaded random polycrystalline SURMOF films grown on insulating borosilicate glass. (b) I - V characteristic of pristine random polycrystalline SURMOF film grown on borosilicate glass. Infiltration with TCNQ molecules and the concomitant increase in carrier density greatly improves the lateral in-plane electrical conductivity of polycrystalline SURMOF films. In both cases the borosilicate glass substrates were not functionalized with Au and SAMS and therefore resulted in random polycrystalline MOF films. However, only the TCNQ loaded SURMOF films with higher carrier density grown on glass produce random polycrystalline films that allow the majority charge carrier hole transport through any directions, reference [28].

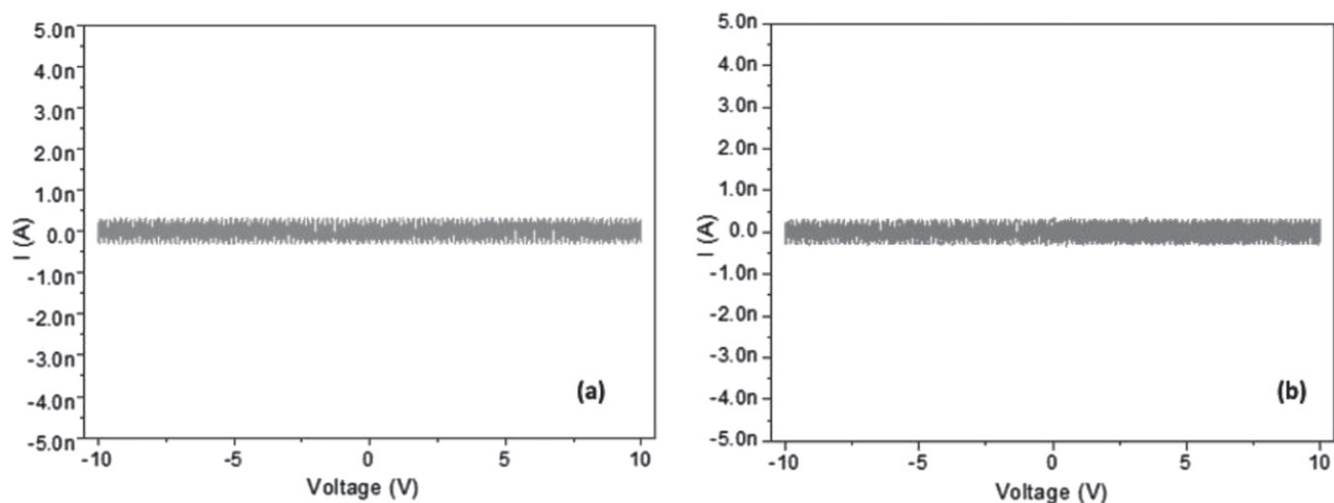


Figure 9. (a) Plot of I - V characteristics of preferentially (001) oriented pristine (undoped) MOF films grown on surface functionalized quartz. (b) I - V characteristic of preferentially oriented SURMOF films grown on functionalized quartz substrates and loaded with TCNQ resulting in increased carrier density. Basically, there is no difference in lateral in-plane electrical conductivity between pristine and TCNQ loaded MOF samples, when the MOF films are preferentially oriented. In both cases there is no measurable lateral in-plane current, because of crystal orientation dependence of electrical conduction, reference [28].

I - V curve indicates good Ohmic conduction. For comparison and in stark contrast, the I - V curve of preferentially (001) oriented MOF films grown on quartz substrates reveal in figure 9, that TCNQ loading with the concomitant increase in carrier density cannot affect any horizontal in-plane electrical conduction for the case of all preferentially oriented SURMOF films. Both TCNQ loaded and pristine SURMOF films show lateral in-plane current of zero measured in the voltage range from -10 V to 10 V. These results corroborate the Seebeck results and further demonstrate that these preferentially (001) oriented SURMOF films exhibit a large electrical anisotropy with no charge carrier transport in the horizontal direction parallel to

the sample surface, but only carrier transport in the vertical direction from front to backside, where switching effects have been reported [11]. The SURMOF films grown on borosilicate glass without any surface functionalization produce random polycrystalline films that allow the majority charge carrier hole transport horizontally through the film between two contacts, because the randomness ensures sufficient numbers of grains with the crystallographic orientation that conduct electrical current.

In order to further confirm the accuracy and reproducibility of the four-point Van der Pauw measurements a new set of SURMOF films were subsequently synthesized on hydroxyl

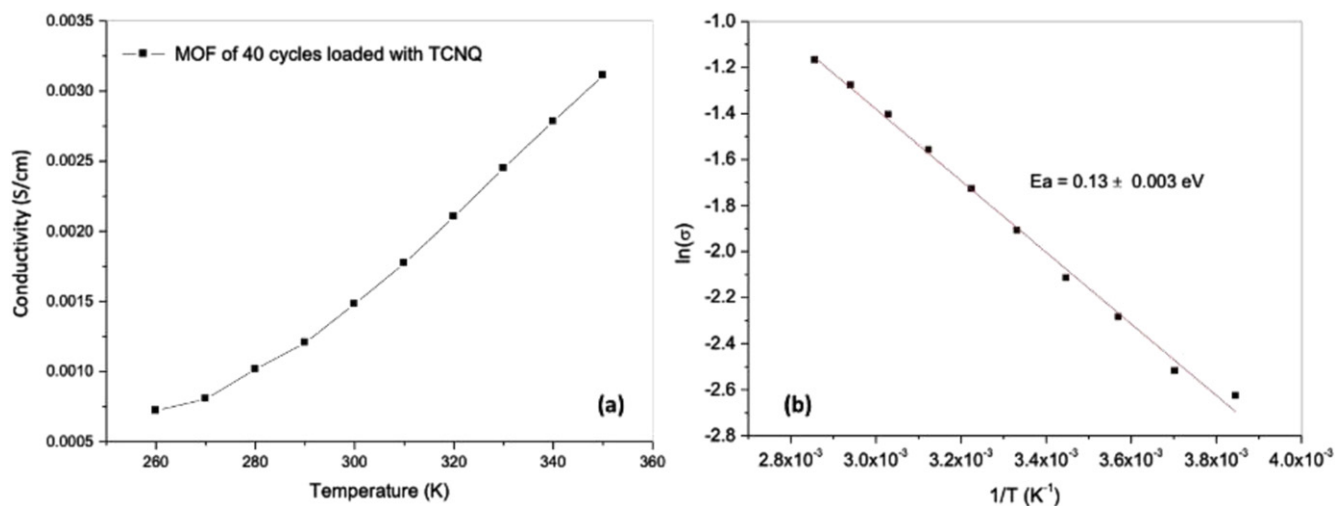


Figure 10. (a) Plot of temperature dependence of electrical conductivity σ of TCNQ loaded MOF grown on borosilicate glass substrate. (b) Arrhenius plot of $\ln(\sigma(T))$ versus T^{-1} . These measurements were performed on MOF films of ~ 130 nm thickness grown on borosilicate glass substrate by an Ecopia HMS-5300 measurement system, reference [28].

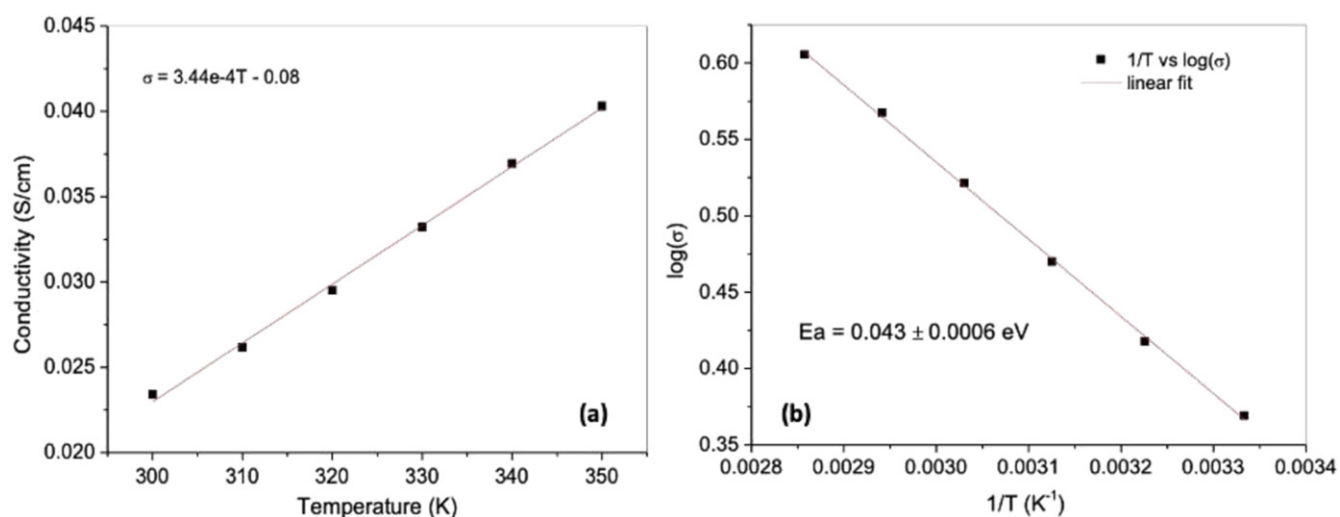


Figure 11. (a) Plot of the electrical conductivity σ as a function of temperature of TCNQ loaded SURMOF film grown on thick 40 nm isolation SiO₂ covered Si substrates. (b) Arrhenius plot of $\ln(\sigma(T))$ versus T^{-1} , reference [28].

terminated native oxide covered Si substrates in the same way as the ones studied in the previous section and the texture and morphology was compared with the films grown on borosilicate glass substrates. Figure 4 displays planar view FE-SEM micrographs of MOF films grown on borosilicate glass substrates showing pristine MOFs and TCNQ loaded MOFs of 10 cycles and 40 cycles resulting in thickness of ~ 40 nm and ~ 130 nm. However, the MOF films grown on borosilicate glass substrate exhibit a loosely stacked granular surface morphology with considerable gaps between the individual MOF grains. The MOF film morphology obtained on borosilicate glass substrates is in contrast with the more dense and compact SURMOF films grown on hydroxyl terminated native oxide covered silicon substrates, shown in figure 5, where all the MOF grains are in direct physical contact forming a continuous compact film thereby creating a good electrical connection shown in figure 11. This morphological difference is

attributed to the lack of proper surface wetting by lacking hydroxyl surface termination and inferior chemisorption of the LPE sprayed MOF film on borosilicate glass.

The investigation of the temperature dependence of the electrical conductivity σ of random polycrystalline MOF films of ~ 130 nm thickness grown on insulating borosilicate glass substrates in the temperature range of 260–350 K is shown in the plot of figure 10(a). The electrical conductivity σ increases as a function of rising temperature, which is attributed to thermal activation generating more majority charge carriers in the SURMOF film. Interestingly, this temperature dependent electrical conductivity behavior indicates semiconductor-like conductivity as opposed to metal conductivity behavior. As temperature increases from 260 K to 350 K, the electrical conductivity of TCNQ loaded MOF increases from 7.129×10^{-4} S cm⁻¹ to 3.1×10^{-3} S cm⁻¹. The results are consistent with reported works [15, 16]. The low

electrical conductivity of MOF films grown on borosilicate glass substrates results from the activation energy of the sample, which can be calculated from the slope of $\sigma(T)$ vs $1/T$ curve shown in figure 10(b) based on $\sigma \sim \exp(E_a/T)$. The red line represents a linear fit that represents a thermally activated process where the sample shows a near-linearly relationship between electrical conductivity and the reciprocal of temperature over temperature range of 300–350 K with an activation energy E_a of 0.13 eV, which is slightly above reported values of 0.052 eV [15]. For benchmarking the electrical conductivity over the temperature range of 260–350 K of polycrystalline SURMOF films grown on 40 nm thick thermal isolating SiO₂ covered Si substrates with bottom Au contacts has been plotted in figure 11(a). In figure 9(b) the red line is linear fit that represents a thermally activated process with an activation energy of 0.043 eV. The slope of the Arrhenius plot can be expressed as E_a/k , where E_a represents activation energy, and k is Boltzmann constant. A low activation energy generally is indicative of a higher charge carrier density and hence higher electrical conductivity. The activation energy E_a of SURMOF films grown on thick amorphous isolating SiO₂ on Si substrates is smaller compared to the SURMOF films grown on borosilicate glasses, indicating the SURMOF films grown on SiO₂/Si substrates exhibit a higher electrical conductivity. This is attributed to morphological differences between relatively loosely stacked and more porous SURMOF films grown on borosilicate glass versus compact and dense MOF films grown on hydroxyl terminated SiO₂ interfaces on Si substrates highlighted in the SEM micrographs of figures 4 and 5. The chemistry of the growth interface exerts a considerable influence on the resulting morphology of SURMOF HKUST-1 film by providing better chemisorption and better surface wetting of the precursor chemicals by providing saturated nucleation sites. In a separate study Wilmer *et al* demonstrated that infiltration of the pores in SURMOF films with absorbates also affects thermal transport by introducing additional phonon scattering in HKUST-1 SURMOF films thereby greatly lowering thermal diffusivity and reducing thermal conductivity in HKUST-1 films [25].

Recent advances in another MOF category of e.g. layered Ni₃(2,3,6,7,10,11-hexamino-triphenylene)₂ (Ni₃(HITP)₂) [26] MOGs (molecular-organic graphene) report significant increases in electrical conductivity, which looks promising for future reliable Hall analysis.

Furthermore, we attempted first Hall effect measurements in the temperature range of 260–350 K in order to establish the critical electrical parameters like Hall coefficient, the Hall mobility and the carrier density to complete a comprehensive electrical characterization of HKUST-1 SURMOF films. The generally positive Hall coefficient of all investigated MOF films indicate, that the MOF films are *p*-type and the positive charge carriers are holes, which is consistent with previous work [26] and thus provides an independent confirmation of our Seebeck results on the carrier type. In spite of electrical conductivities of $\sim 3.1 \times 10^{-3}$ S cm⁻¹ at 350 K in SURMOF films on borosilicate substrates, the contact resis-

tances of our HKUST-1 samples were measured in excess of 1–2 M Ω , which prevent reliable Hall measurements at a magnetic field of 0.55 T. Subsequently the Hall measurements were repeated at an external lab in much higher magnetic fields from 1 T to 6 T using a PPMS quantum design physical property measurement system [27]. However even at a magnetic field of 6 T the MOhm contact resistant between the bottom Au contacts and HKUST-1 SURMOF film proved too high for reproducible Hall measurements [28]. As future outlook and perspective, we have to summarize that the current generation of TCNQ loaded HKUST-1 requires better contact technology and much improved doping techniques to achieve lower contact resistances in order to enable reproducible Hall measurements.

In this context, Maissa Barr, Bachmann *et al* at Friedrich-Alexander Universität Erlangen-Nürnberg, Germany, have recently shown a promising new approach of achieving for the first time solution-based atomic layer deposition (s-ALD) [29] synthesis of Cu-BDC MOF films, which could offer in the future hitherto totally unknown technical possibilities of *in situ* doping of growing MOF films. As a perspective such successful demonstration of solution based ALD (s-ALD) technology of crystalline MOF films opens up the prospect of precise Angstrom film thickness control of true conformal layer-by-layer growth of MOF films with superior control of smooth surface morphology, which is a prerequisite for large volume industrial scale technological applications ranging from sensors, batteries, fuel cells and photovoltaic devices as well as to functional thin film materials in the field of electrochemistry, optoelectronics, luminescence, up-conversion, proton conductivity, optics and photonics, thermoelectrics, sensing, magnetism, non-linear optics, data storage as well as to photo-/electrocatalysis, membranes, chemical reactors and gas storage.

2. Summary

In conclusion, we report experimentally determined electrical characterization to demonstrate different electrical properties for pristine HKUST-1 and TCNQ loaded HKUST-1 SURMOF films while benchmarking compact random polycrystalline SURMOF films versus preferentially (001) oriented films grown by the LPE spray method. In addition, the electrical conductivity as well as the Seebeck coefficient has been investigated in detail. In our study HKUST-1 MOF thin films have been grown using LPE on surface functionalized and modified silicon and on borosilicate glass substrates. The resulting MOF thin films have been further doped with TCNQ molecules. Pristine and TCNQ loaded samples of monolithic HKUST-1 SURMOF thin films with a thickness of ~ 130 nm has been carefully investigated by Seebeck analysis and current–voltage (*I–V*) measurements. Our investigation reveal crystal orientation dependent anisotropic electrical conductivity. Such (001) preferentially oriented crystalline SURMOF films exhibit only vertical electrical conduction between front and backside contacts of the

SURMOF film, whereas there is no measurable horizontal in-plane conductivity between either two or four surface contacts. However, very dense compact and isotropic random polycrystalline MOF films have demonstrated surprisingly high in-plane electrical conductivity between van der Pauw sample surface contacts.

These fundamental Van der Pauw sample configuration measurements provide important insights into the anisotropy of electrical conduction and electrical characteristics of these materials, which renders these MOF films attractive for upcoming microelectronic and optoelectronic applications. It is foreseeable that the anisotropy of the electrical conductivity in crystalline SURMOF films lends itself readily to be advantageously exploited for electronic applications. At the current stage of materials development, the contact resistance of HKUST-1 SURMOF films are still too high to render reproducible Hall measurements feasible for a comprehensive electrical characterization. In perspective, more work in this stimulating field is required. In particular, the doping technology of SURMOF films must be improved dramatically to increase the carrier density and electrical conductivity and to improve the contact resistance.

There is no fundamental roadblock to prevent further steady materials improvement as this materials class possesses outstanding and tunable electrical properties for highly conductive SURMOF thin film materials and coatings. Based on this initial electrical characterization work we anticipate a promising future of SURMOF films with good potential in the future initially in thermoelectric applications and with improved electrical conductivity later on in microelectronic systems applications.

Acknowledgments

ER is thanking the DFG, KIT and CMM for sustainable research funding. This work was funded within the priority program SPP 1362 and SPP 1928 of the German Research Foundation (DFG). The authors would like to acknowledge the College of William and Mary (Williamsburg, Virginia) for the use of the FE-SEM and California State University Los Angeles for the Quantum Design PPMS experiments.

Data availability statement

All data that support the findings of this study are included within the article (and any supplementary files).

ORCID iDs

Engelbert Redel  <https://orcid.org/0000-0001-7687-5637>

References

- [1] (a) Bittle E G, Basham J I, Jackson T N, Jurchescu O D and Gundlach D J 2016 *Nat. Commun.* **7** 10908
(b) Hunter S, Ward J W, Payne M M, Anthony J E, Jurchescu O D and Anthopoulos T D 2015 *Appl. Phys. Lett.* **106** 223304
- [2] (a) Li H, Eddaoudi M, O'Keeffe M and Yaghi O M 1999 *Nature* **402** 276–9
(b) Yaghi O M, Li G M and Li H L 1995 *Nature* **378** 703–6
- [3] Ferey G and Serre C 2009 *Chem. Soc. Rev.* **38** 1380–99
- [4] Shekhah O, Liu J, Fischer R A and Wöll C 2011 *Chem. Soc. Rev.* **40** 1081–106
- [5] Liu J et al 2012 *Sci. Rep.* **2** 921
- [6] Shekhah O et al 2007 *J. Am. Chem. Soc.* **129** 15118
- [7] Bundschuh S, Kraft O, Arslan H K, Gliemann H, Weidler P G and Wöll C 2012 *Appl. Phys. Lett.* **101** 101910
- [8] Best J P et al 2015 *Appl. Phys. Lett.* **107** 101902
- [9] (a) Hermes S, Schroder F, Chelmowski R, Wöll C and Fischer R A 2012 *J. Am. Chem. Soc.* **127** 13744–5
(b) Biemmi E, Scherb C and Bein T 2007 *J. Am. Chem. Soc.* **129** 8054–5
(c) Horcajada P, Serre C, Grosso D, Boissiere C, Perruchas S, Sanchez C and Ferey G 2009 *Adv. Mater.* **21** 1931–5
- [10] Gliemann H and Wöll C 2012 *Mater. Today* **15** 110–6
- [11] Wang Z et al 2016 *ChemNanoMat* **2** 67–73
- [12] Yoon S M, Warren S C and Grzybowski B A 2014 *Angew. Chem., Int. Ed.* **53** 4437–41
- [13] Dragässer A, Shekhah O, Zybaylo O, Shen C, Buck M, Wöll C and Schlettwein D 2012 *Chem. Commun.* **48** 663–5
- [14] Talin A A et al 2014 *Science* **343** 66
- [15] Neumann T et al 2016 *ACS Nano* **10** 7085–93
- [16] Erickson K J et al 2015 *Adv. Mater.* **27** 3453–9
- [17] Arslan H K, Shekhah O, Wohlgenuth J, Franzreb M, Fischer R A and Wöll C 2011 *Adv. Funct. Mater.* **21** 4228–31
- [18] Liu J et al 2015 *Chem. Mater.* **27** 1991–6
- [19] Silvestre M E, Franzreb M, Weidler P G, Shekhah O and Wöll C 2013 *Adv. Funct. Mater.* **23** 1210–3
- [20] Huang X et al 2015 *Nat. Commun.* **6** 7408
- [21] Chen X, Wang Z, Lin P, Zhang K, Baumgart H, Redel E and Wöll C 2016 *ECS Trans.* **75** 119–26
- [22] Chen X, Wang Z, Hassan Z M, Lin P, Zhang K, Baumgart H and Redel E 2017 *ECS J. Solid State Sci. Technol.* **6** P150–3
- [23] Redel E and Baumgart H et al 2020 *APL Mater.* **8** 060902
- [24] Babaei H et al 2020 *Nat. Commun.* **11** 4010
- [25] Van der Pauw L J 1958 *Philips Tech. Rev.* **20** 220–4
- [26] (a) Sun L et al 2017 *Joule* **1** 167
(b) Sun L, Campbell M G and Dincă M 2016 *Angew. Chem., Int. Ed.* **55** 3566–79
- [27] Truong B and Zhao G-M 2019 *Private Communication, MOF Hall Coefficient Measurements Using Quantum Design PPMS* (Los Angeles, USA: Department of Physics and Astronomy, California State University)
- [28] Chen X 2017 *Dissertation* Norfolk, Virginia Old Dominion University
- [29] Barr M K S et al 2020 Atomic layer deposition from dissolved precursors—solution ALD (sALD), abstract Nr. H05-142750 *2nd Int. Symp. H05: Metal Organic Frameworks (MOFs) Covalent Organic Frameworks (COFs) and Porous Hybrid Materials: Characterization, Technology, Bio-Applications, and Emerging Devices at the ECS PRIME 2020* (Honolulu, Hawaii: Fall Meeting of the Electrochemical Society)